Mechanism of Site-Specific Psoralen Photoadducts Formation in Triplex DNA Directed by Psoralen-Conjugated Oligonucleotides†

Yueh-Hsin Ping‡ and Tariq M. Rana*

Department of Biochemistry and Molecular Pharmacology, University of Massachusetts Medical School, Worcester, Massachusetts 01605

Received June 2, 2004; Revised Manuscript Received October 6, 2004

ABSTRACT: Triplex-formation oligonucleotides attached with a photoreactive psoralen molecule (psoTFO) can be used to induce site-specific DNA damage and to control gene expression. Inhibition of transcription by psoralen-cross-linked triplexes results in both arrest and termination of RNA Pol II transcriptional complexes during elongation. To understand the relationship between triplex psoralen cross-linking products and the fate of RNA Pol II elongation complexes, it is important to delineate the mechanism for creating site-specific psoralen photoadducts in a target duplex DNA. To investigate the mechanism of photoadduct-formation by psoralen photo-cross-linking, triplex structures were generated by targeting a DNA duplex with psoTFOs of different lengths. The psoralen photoadducts were then analyzed after UV irradiation, which initiates the psoralen cross-linking reaction. Our results demonstrated that UV irradiation of triplexes formed between a psoTFO and a DNA duplex generated two distinct groups of psoralen photoadducts: monoadducts and psoralen interstrand cross-link products. The formation of these psoralen photoadducts was also photoreversible through exposure to short wavelength UV irradiation. The length of a psoTFO was shown to establish the position at which psoralen was added to the target DNA duplex and determined which photoadducts products formed predominantly. Kinetic experiments that monitored the formation of the psoralen photoadducts also suggested that the length of the psoTFO influenced which photoadducts were preferentially formed at faster rates. Taken together, these studies provide new insight into the mechanism associated with the formation of psoralen photoadducts that are directed by psoTFO during triplex formation.

Triple-stranded helical DNA has been extensively studied in light of its potential roles in various biological processes, including regulation of gene expression. The structure and formation of triplexes has also been analyzed, providing some insight into its possible niches in vivo. Triplexes are formed when single-stranded DNA interacts with double-stranded DNA within the major groove (*1*). Formation of triplex structures requires Watson−Crick base-pairing established by hydrogen bonding within duplex DNA. The third strand then forms the triplex through Hoogsteen base pairing on another surface of the duplex (*2*). Another requirement for triplex formation is that the central strand of the triplex has to be a purine rich stretch of nucleotides as pyrimidines do not have two hydrogen-bonding surfaces to form a stable triplex structure.

There are at least two major structural motifs of intermolecular triple helices that exist and they differ by both the sequence composition of the third strand and the relative orientation of the phosphate-deoxyribose backbones. The pyr·pur−pyr structural motif shows an oligopyrimidine third strand whose backbone orientation is parallel to that of the target purine tract that interacts through Hoogsteen hydrogen bonds to form T·A−T and C^+·G−C triads (*3*−*5*). C^+·G−C triads are stably formed only at low pH (<6.0) because protonation of the third strand cytosine is required to stabilize the triplex. However, this motif can be stabilized at neutral pH when cytosines on the third strand are replaced with 5-methylcytosines (*6, 7*). Addition of a single 5-methylcytosine in a stretch of thymidine residues is known to stabilize the triplex structure because it recognizes a single G·C base pair in a poly A·T sequence (*8*). In the pur·pur−pyr motif, an oligopurine third strand whose backbone orientation is antiparallel to the purine tract interacts through reverse Hoogsteen hydrogen bonding to form A·A−T and G·G−C triads (*9*−*11*). Triplex structures are often formed with triplex-formation oligonucleotides (TFO),[1] which are single-stranded oligonucletodes having the capacity to bind double-stranded DNA helices to form the triple helix. TFOs have been proposed to be DNA-specific ligands and oligonucleotide-directed triple-helix formation has developed into one of the most versatile approaches to targeting sequences of specific double-helical DNA and controlling gene expression (*12*−*14*).

† This work was supported in part by grants from the NIH (AI 41404 and AI 43198).

* To whom correspondence should be addressed: Chemical Biology Program, Department of Biochemistry and Molecular Pharmacology, University of Massachusetts Medical School, 364 Plantation St., Worcester, MA 01605. Telephone: 508-856-6216. Fax: 508-856-6696. E-mail: tariq.rana@umassmed.edu.

‡ Present address: Institute of Pharmacology, National Yang-Ming University, Shih-Pai, Taipei 11221, Taiwan.

[1] Abbreviations: TFO, triplex-forming oligonucleotides; Pso, psoralen; psoTFO, psoralen modified triplex-forming oligonucleotides; LTR, long terminal repeat.

10.1021/bi0488707 CCC: $30.25
Published on Web 01/25/2005

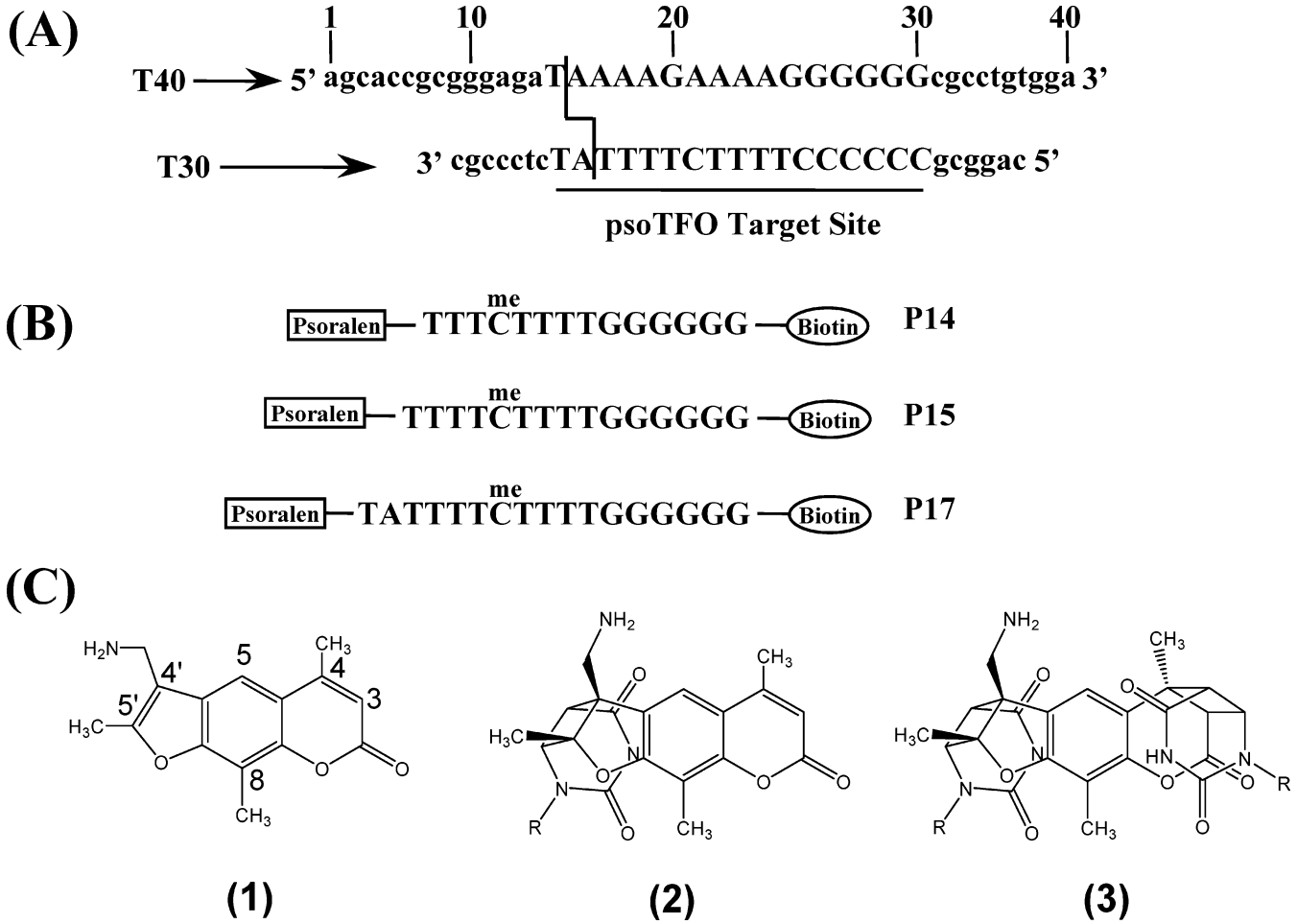

FIGURE 1: Structure of the DNA duplex target and psoTFOs. (A) The sequences of two single strands of DNA, T40 and T30, were used to form a DNA duplex. The capital letters in the sequence represent the targeting site of the psoTFO. (B) Three psoTFOs that varied in length were synthesized to target the DNA duplex and form triplex complexes. All three psoTFOs were conjugated with a psoralen molecule at the 5′-end and a biotin molecule at the 3′-end. Cytosine residues in the sequences of the psoTFOs were substituted with 5-methylcytosine as indicated to stabilize triplex structure (*6, 14*). (C) Structures of the two types of 4′-aminomethyl-4,5′,8-trimethylpsoralen (AMT)−uridine adducts formed by the photoreaction of AMT with RNA: (1) AMT; (2) furan-side monoadduct; (3) furan-side and pyrone-side diadduct.

Attachment of psoralen to a nucleic acid binding molecule creates an efficient nucleic acid cross-linking molecule. Psoralens are bifunctional photoreagents that have been used as photoactive probes of nucleic acid structure and function (*15*). Psoralens intercalate between base pairs of double stranded nucleic acids. Upon ultraviolet irradiation (320−400 nm), the intercalated psoralens photoreact with adjacently stacked pyrimidine bases to form a pyrimidine-psoralen monoadduct (*16, 17*). Typical photoreactions of a psoralen are shown in Figure 1C. Psoralens form two kinds of monoadducts: the furan-side monoadduct, M_{Fu}, which is formed through the cycloaddition between the 4′,5′ double bond of psoralen and the 5,6 double bond of a pyrimidine base; and the pyrone-side monoadduct, M_{Py}, which is formed through the cycloaddition between the 3,4 double bond of a psoralen and the 5,6 double bond of a pyrimidine base (Figure 1C). Oligonucleotides carrying psoralen at a specific site in the sequence are powerful tools for molecular biology and could provide a new class of therapeutic agents (*18, 19*). Photochemical properties of psoralens can be exploited to generate DNA probes containing psoralen monoadducts at specific sites, and these probes can form site-specific cross-links to the complementary target sequences (*20, 21*). Psoralen-modified oligonucleotides have been used to trap three-stranded RecA-DNA complexes and to study the repair of these cross-linked complexes (*22, 23*). It has also been shown that psoralen-derivatized oligodeoxyribonucleotides and oligoribonucleoside methylphosphonates can specifically cross-link to double-helical DNA and viral mRNA targets, respectively (*24, 25*).

Psoralen can be used to probe both static and dynamic helical structures since short-lived nucleic acid interactions can be stabilized through the formation of covalent psoralen cross-links. Previous studies have utilized psoralen to characterize the interactions between nucleic acids as well as protein-nucleic acid interactions (*26−29*). In addition, several in vivo studies have demonstrated that psoralen cross-links can be introduced and detected within human cells and that the DNA repair of triplex helix-directed psoralen damage in vivo was not very efficient (*30−33*). Recently, TFO covalently linked to psoralen (psoTFO) have been used to target specific DNA sequences in cell-free or intracellular systems, causing significant biological consequences that included transcriptional inhibition and mutagenesis (*13, 34−36*). To study the dynamics of transcriptional activation in HIV-1 LTR promoter, our laboratory developed a new biochemical method to isolate RNA polymerase II elongation complexes by introducing site-directed psoralen cross-links

to a DNA template containing the HIV-1 LTR promoter (*37*). Results from these experiments showed that DNA damage resulting from psoralen cross-links could cause RNA Pol II transcription complexes to arrest or terminate transcription altogether (*37*).

In this study, a model DNA duplex was used as the target of psoralen-conjugated TFOs to elucidate the fundamental photochemistry involved in the formation of psoTFO-duplex cross-links. Three psoTFOs of different lengths were synthesized and site-specific photo-cross-linking reactions were performed in the presence of the DNA duplex target. Our results demonstrated that UV irradiation of triplexes formed between a psoTFO and a DNA duplex generated two distinct groups of psoralen photoadducts: monoadducts and psoralen interstrand cross-link products. Furthermore, our analysis demonstrated that psoTFOs are able to direct psoralen to specific DNA targets and that the position of psoralen can determine the chemical nature of the photoadducts. The formation of these psoralen photoadducts was also photoreversible through exposure to short wavelength UV irradiation. Finally, the data presented here suggested that the length of the psoTFO can influence the position of the psoralen cross-linking site on the target DNA duplex and the kinetics of formation of various monoadduct and psoralen interstrand cross-link products. Altogether, this study suggested that both sequence and length of psoTFo was important for the formation of psoralen cross-linking products, shedding light on the mechanisms involved with psoralen photochemistry and triplex formation.

MATERIALS AND METHODS

Buffers. All buffer pH values refer to measurements at room temperature. *TBE buffer:* 45 mM Tris-borate at pH 8.0, and 1 mM EDTA. *Sample loading buffer:* 9 M urea, 1 mM EDTA, and 0.1% bromophenol blue in 1x TBE buffer. *Triplex binding buffer (TBB):* 10 mM Tris−HCl at pH 7.0, 50 mM NaCl, 10 mM $MgCl_2$, and 0.5 mM spermine. *T4 kinase buffer:* 70 mM Tris−HCl at pH 7.5, 10 mM $MgCl_2$, and 5 mM DTT. *DNase I digestion buffer:* 10 mM Tris−HCl, pH 7.4, 50 mM $MgCl_2$, 50 mM $CaCl_2$, and 5% glycerol.

Synthesis of Oligonucleotides. The sequences of duplex DNA and the third strand probes containing psoralen at the 5′-end and biotin at the 3′-end are shown in Figure 1. Synthesis, purification, and characterization of the third strand probes were accomplished according to previously described methods (*17*, *37*). The psoTFO target site shown in Figure 1A represents the position that the third strand TFO binds to DNA duplex to form DNA triplex helix. All DNAs were synthesized on an Applied Biosystems ABI 392 DNA/RNA synthesizer, deprotected in NH_4OH at 55 °C for 8 h, and then dried in a Savant speed-vac. DNA oligonucleotides were resuspended in sample loading buffer and were purified on 20% polyacrylamide/7 M urea gel. Concentration of DNA oligonucleotides was determined by measuring absorbance at 260 nm in a Shimadzu UV spectrophotometer. The DNAs T30 and T40 used to form the DNA duplex, were 5′-end-labeled with 0.5 μM, [γ-^{32}P]ATP (6000 Ci/mmol) (ICN) per 100 pmol of DNA by incubating 16 units of T4 polynucleotide kinase (NEB) in T4 kinase buffer at 37 °C for 45 min. After kinase reactions, the concentration of DNA was adjusted to 2 μM.

Formation of DNA Duplex. DNA duplex target containing TFO binding sites was formed by annealing two complementary single strands of DNA, T30 and T40, shown in Figure 1A. Equimolar quantities of complementary oligonucleotides were mixed in TBB, heated at 95 °C for 3 min, and then gently cooled to room temperature over 30 min.

Triplex Formation and Photo-Cross-Linking Reactions. DNA duplex (0.2 μM final concentration) was incubated with excess psoralen-conjugated probe (x 500, 50 μM final concentration) in TBB for 30 min at 37 °C, and cooled slowly to 0 °C (*37*). The reaction mixture was irradiated with UV (360 nm) on ice in a Photochemical Reactor (Rayonet RPR 100) for 15 min. For photoreverse reactions, the reaction mixture was irradiated with UV (254 nm) on ice for 5 min. After UV irradiation, 20 μL of sample loading buffer were added. The reaction mixtures were heated at 85 °C for 3 min before being loaded on 10% polyacrylamide/7M urea gels.

DNase I Footprinting. The condition of DNase I digestion was adapted from published procedures with minor modification (*38*, *39*). The ^{32}P-labeled psoralen cross-linking products were purified from the gel and resuspended in DNase I digestion buffer. Footprinting reactions were initiated by addition of DNase I (0.8 units/mL) and allowed to proceed at room temperature for 3 min. The reactions were terminated by addition of 10 mM EDTA and sample loading buffer followed by heating to 95 °C for 5 min. The DNA fragments were analyzed on 20% polyacrylamide/7 M urea gels. Maxam−Gilbert sequencing reactions (C), (C+T), (G), and (A+G) of the DNA duplex fragment were performed and analyzed on the same gel as the DNase I digest for sequence determination.

RESULTS

The length of psoTFOs is an important determinant of photoproduct formation during psoralen photo-cross-linking reactions. Previous studies have shown that the inhibition of transcription by psoralen-cross-linked triplexes resulted from both arrest and termination of RNA Pol II transcriptional complexes during elongation (*37*). To understand the relationship between triplex psoralen cross-linking products and the fate of RNA Pol II elongation complexes, it is important to delineate the mechanism for creating site-specific psoralen photoadducts in a target duplex DNA. To investigate the effect of triple-helix-formation by psoralen UV-cross-linking, we synthesized two single strands of DNA, T40 and T30, to be used in the formation of a DNA duplex (Figure 1A). Our third strand probes are capable of binding in parallel orientation to the polypurine sequence in target duplex DNA where T recognizes A·T base pairs to form T·A·T base triplets and G recognizes G·C base pairs to form G·G·C base triplets (*8*). In addition, a single 5-methylcytosine was incorporated in the sequence to stabilize the triplex structure. Incorporation of a single 5-methylcytosine in a stretch of T residues is known to enhance the stability of triplex DNA (*8*). The third-strand DNA probes used as TFOs were conjugated with a psoralen molecule at the 5′-end that can covalently link with the DNA duplex and a biotin molecule at the 3′-end that binds with streptavidin-coated magnetic beads. Three psoralen-conjugated TFOs (psoTFO) of varying lengths, P14, P15, and P17 (14, 15, and 17,

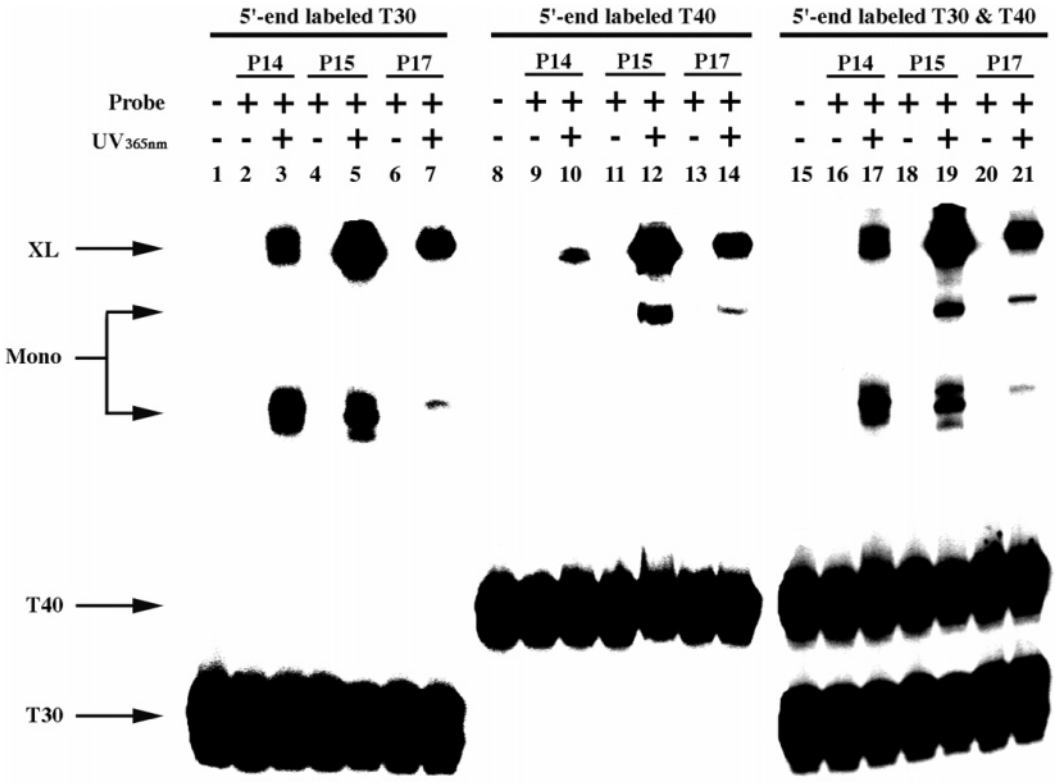

FIGURE 2: Formation of psoralen photo-cross-linking products. Reactions were carried out using different 5′-end ^{32}P-labeled strands of DNA duplex, T30 (lanes 1−7), T40 (lanes 8−14), and both T30 and T40 (lanes 15−21). Triplex complexes were generated after DNA duplexes were bound to one of the three psoTFOs, P14 (lanes 2, 3, 9, 10, 16, and 17), P15 (lanes 4, 5, 11, 12, 18, and 19), or P17 (lanes 6, 7, 13, 14, 20, and 21), respectively. Lanes 1, 8, and 15 are duplex DNA alone. T30 and T40 represent the 5′-end ^{32}P-labeled strands of DNA duplex. Mono indicates bands containing monoadducts. XL indicates bands containing psoralen interstrand cross-links. For experimental conditions, see Materials and Methods.

respectively, equal the number of nucleotides in the psoTFO), were synthesized to study the effect of the length of DNA oligonucleotides targeting a DNA duplex on triplex formation (Figure 1B). As shown in Figure 1B, the three psoTFOs contain the same sequences at the 3′-end but vary in length at the 5′-end where the psoralen molecule was conjugated at the 5′-end of the TFO. Therefore, the length of the psoTFO determines the position where psoralen cross-links with the DNA duplex target. In addition, cytosine residues within the sequence of the TFOs were substituted with 5-methylcytosine to stabilize triplex structure at neutral pH condition (*6*, *7*).

A 30 base-paired DNA hetroduplex fragment was formed by mixing two single-stranded DNA oligonucleotides, T30 and T40. The DNA duplex formed contains either only one or both DNA strand(s) radioactively labeled. DNA triplexes were formed by the binding of the psoTFO with DNA duplex and then were psoralen cross-linked through two successive photochemical reactions using UV irradiation at wavelength 365 nm. Two pools of cross-linked species were expected to form through this process. Monoadducts resulted from psoralen covalently cross-linking with only one single strand of duplex and will migrate slower than free single-stranded DNA on a denaturing gel. In contrast, interstrand cross-links arise from covalent linkages between psoralen and two strands of DNA, and migrate the slowest on a denaturing gel.

To examine how psoralen covalently links to the DNA duplex, we end-labeled DNA duplex by [γ-^{32}P] ATP on either only one or both strands of duplex. Our results showed that all three probes were able to form cross-link products with the DNA duplex after UV irradiation and as expected, two distinct bands, representing the two groups of slowly migrating species of labeled DNA, were detected (Figure 2, lanes 3, 5, 7, 12, 14, 17, 19, and 21). When single-stranded T30 or T40 strands were labeled, the cross-linking products of all three probes were detected. With the T30 strand, psoralen monoadducts were also formed with all three psoTFOs (Figure 2, lanes 3, 5, and 7). However, T40 only formed monoadducts with probe P15 and P17 (Figure 2, lanes 12 and 14), with no monoadducts being detected when P14 was used as a psoTFO with T40 (Figure 2, lane 10). Products similar to those seen with T30 labeling were also observed when both DNA strands were labeled, but the pool of the different migrating species varied among the psoTFOs (Figure 2, lane 17, 19, and 21). P14 gave rise to monoadducts with the T30 strand as major products and lower yields of psoralen interstrand cross-link products. On the other hand, P15 gave psoralen interstrand cross-links as major products and monoadducts as minor products. P17, composed of only two more nucleotides than P15, mostly formed psoralen interstrand cross-links with only a very small pool of monoadducts detected. These results indicated that varying the length of psoTFOs relative to the position of psoralen to the cross-link site on DNA duplex can generate different products of psoralen photoadducts.

The formation of psoralen photo-cross-link products is reversible by short wavelength UV irradiation. To determine the chemical nature of the photoadducts resulting from covalent linkage of psoralen with the DNA duplex, we took advantage of the reversibility of psoralen cross-linking

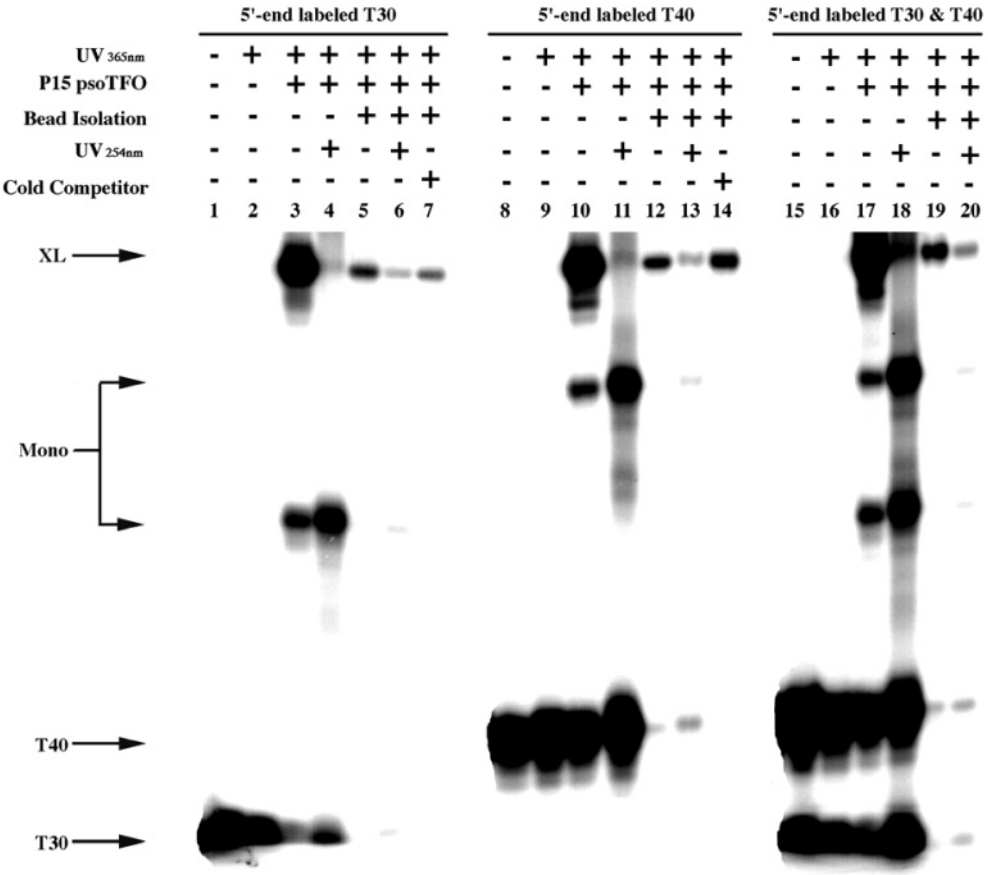

FIGURE 3: Reversibility of psoralen-photo-cross-linked products. P15 psoTFO was bound to the DNA duplex to form triplex complexes as shown in Figure 2. Key: lanes 1−7, labeled T30; lanes 8−14, labeled T40; lanes 15−20, labeled T30 and T40. Lanes 1, 2, 8, 9, 15, and 16 show duplex alone without (lanes 1, 8, and 15) and with (lanes 2, 9, 16) UV irradiation. For lanes 4, 6, 11, 13, 18, and 20, the reaction mixture was irradiated with UV irradiation at 365 nm followed by UV irradiation at 254 nm. Lanes 5−7, 12−14, and 19−20 show the analysis of cross-linking products purified from the reaction mixture after UV irradiation. Lanes 7 and 14 contain excess unlabeled single strands of duplex, T30 (lane 7) and T40 (lane14) to compete with labeled single strands before UV irradiation at 365 nm. T30 and T40 represent the 5′-end ^{32}P-labeled strands of DNA duplex. Mono indicates bands containing monoadducts. XL indicates bands containing psoralen interstrand cross-links. For experimental conditions see Materials and Methods.

photochemistry using UV irradiation at 254 nm (*40*, *41*). P15 was chosen as the psoTFO for this experiment because, as described above, the major products of psoralen cross-linking were interstrand cross-links. Also as performed above, single or double strand radioactively labeled DNA duplexes were used to evaluate cross-link products. After UV irradiation at 365 nm, half of the reaction mixture was further UV irradiated at 254 nm. The resulting gel showed that the psoralen interstrand cross-link products of P15 decreased after UV irradiation at 254 nm while monoadducts and free single strand DNA increased (Figure 3, lanes 3, 4, 10, 11, 17, and 18). These results indicated that the psoralen cross-linking could be reversed, forming both the monoadducts form and free DNA strands upon UV irradiation at 254 nm.

To further demonstrate that the increase in monoadducts arose from the reversal of psoralen cross-linking, cross-link products were isolated from the reaction mixture using streptavidin-coated magnetic beads to bind biotin attached at the 3′-end of the psoTFOs. Purified cross-linked products were then UV irradiated at 254 nm. Consistent with the gel shown in Figure 2, P15, psoralen interstrand cross-links were purified as the major products with DNA duplex with very few monoadducts isolated after UV irradiation at 365 nm (Figure 3, lanes 5, 12, and 19). UV irradiation at 254 nm caused the reversal of cross-linking, resulting in monoadducts and free DNA strands (Figure 3, lanes 6, 13, and 20). To rule out the possibility that monoadducts could result from the third strand probe cross-linking with a single DNA strand alone, unlabeled single stranded DNA was added into reactions to compete with the radiolabeled duplex DNA before UV irradiation at 365 nm. Purification of the cross-linked products from the reaction mixture showed that the level of cross-linking products was not changed compared to the reactions without cold competitors (Figure 3, lanes 5, 7, 12, and 14). These results suggested that both the monoadducts and psoralen interstrand cross-links were only generated after the formation of DNA triplexes prior to UV irradiation at 254 nm. Taken together, these results showed that the psoralen cross-links occurs only when a psoTFO forms a triple helix with the DNA duplex and the cross-links can then be reversed into monoadducts and free DNA strands by short wavelength UV irradiation.

The length of psoTFOs influences the kinetics of psoralen photo-cross-linking reactions. To understand the kinetics of psoralen photoadducts formation, we carried out photochemical reactions for various irradiation time intervals and analyzed the products. Duplex DNA was radioactively labeled on both strands, incubated with one of each of the three probes, and after UV irradiation at 365 nm, cross-linking products were analyzed at different time points. Interestingly,

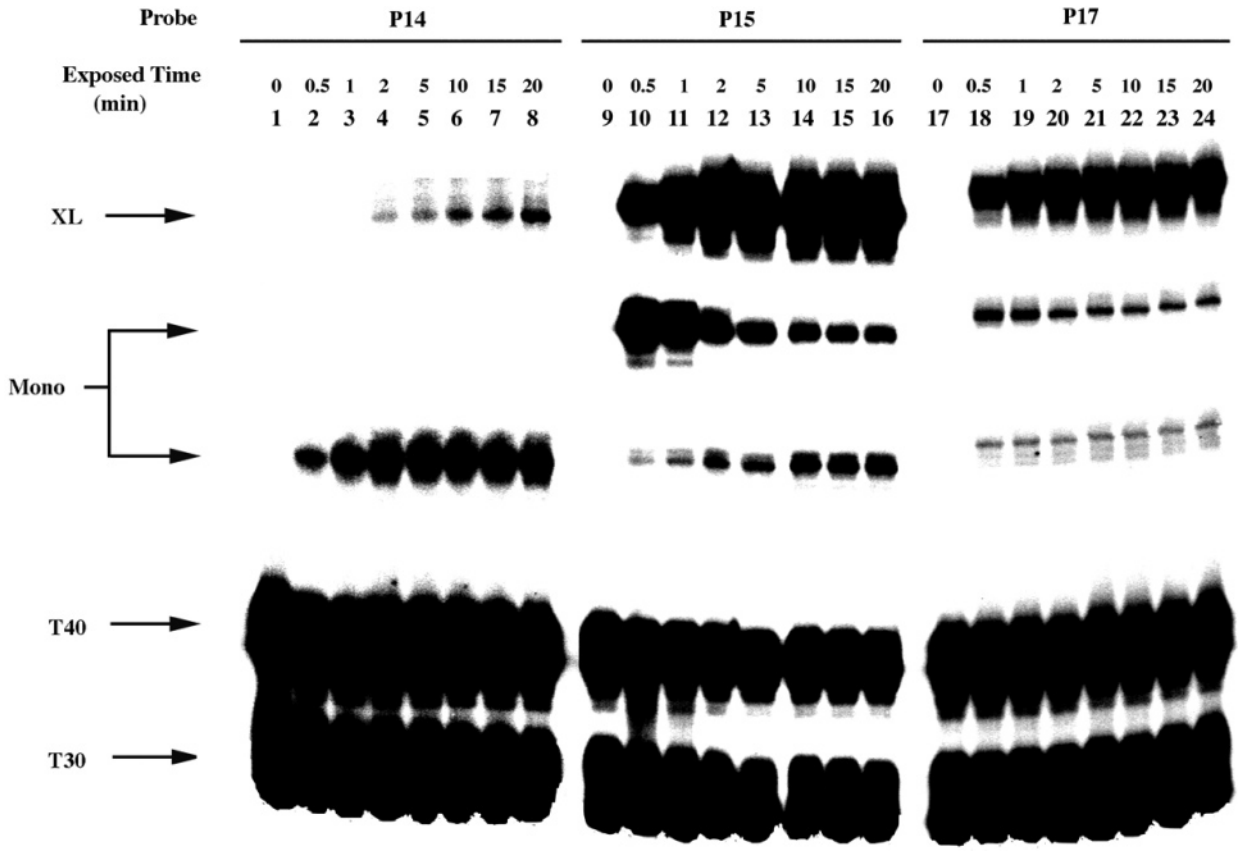

FIGURE 4: Kinetics of monoadduct and interstrand cross-link product formation during psoralen-photo-cross-linking reactions. Triple helixes were generated after DNA duplexes were bound to one of the three psoTFOs P14 (lanes 1−8), P15 (lanes 9−16), or P17 (lanes 17−24), respectively. UV irradiation was carried out within various time periods: Key: lanes 1, 9, and 17 represent UV exposure for 0 min; lanes 2, 10, and 18, 0.5 min; lanes 3, 11, and 19, 1 min; lanes 4, 12, and 20, 2 min; lanes 5, 13, and 21, 5 min; lanes 6, 14, and 22, 10 min; lanes 7, 15, and 23, 15 min; lane 8, 16, and 24, 20 min. T30 and T40 represent the 5′-end ^{32}P-labeled strands of DNA duplex. Mono indicates the monoadducts. XL indicates the psoralen interstrand cross-links.

the three probes showed varying cross-linking photochemistry (Figure 4). The shortest probe, P14, first formed monoadducts with T30 strands right after UV irradiation. The cross-link products of P14 were detected after 2 min exposure with UV irradiation and reached maximum levels of product in 15 min (Figure 4, lanes 1−8). The mid-sized probe, P15, had a dramatically different cross-linking photochemistry compared to P14. Both monoadducts and psoralen interstrand cross-links of P15 were detected after the first 30 s of UV irradiation (Figure 4, lane 10). There was also a decrease in T40 monoadducts concomitant with an increase in psoralen interstrand cross-links, indicating that P15 formed monoadducts with T40 first and then covalently linked to T30 to form cross-links (Figure 4, lanes 10−16). The maximum level of P15 cross-linking occurred within 2−5 min of UV irradiation. P17, the longest probe, showed a cross-linking pattern that was similar to P15 with cross-link products appearing within the first 30 s of UV irradiation (Figure 4, lanes 17−24). However, the cross-links of P17 reached their maximum level by 1 min after UV irradiation, without significant changes in monoadduct products. These results show that the highest yield of interstrand cross-links was obtained with P15 and that P17 was also efficient in forming cross-link adducts with a minimum amount of monoadducts.

Psoralen cross-link sites are formed on 5′-TpA-3′ sequences adjacent to the psoTFO binding site on the target duplex DNA. Psoralen monoadducts and interstrand cross-links are efficiently formed on a target containing 5′-TpA-3′ sequences adjacent to the TFO binding sequence (*42*−*44*). To determine the psoralen photoaddition sites on the T40 and T30 DNA duplex target sequences, a DNase I digestion approach was used. The cross-linking products of P15 were prepared with the T30 or T40 strand radioactively labeled at the 5′-end. The cross-link site was mapped by partial DNase I digestion and by alignment of Maxam−Gilbert sequencing of the end-labeled DNA strand. As shown in Figure 5A and B, base hydrolysis of the labeled DNA strand produced a DNA ladder that resolved all fragments (lane 4). A complete gap indicated the position where the psoralen cross-link site within the hydrolysis ladder of the cross-link product was detected. On T30 strand, the site of the gap is after T21; on T40 strand, the gap occurs after T15 (Figure 5A and B, lane 5). These results demonstrated that P15 psoTFO placed the psoralen molecule at a position near 5′-TpA-3′ sequences and cross-linked to DNA duplex at a 5′-TpA-3′ site on both strands of duplex.

DISCUSSION

Herein, we provide new insight into the mechanism of psoralen photoadducts formation directed by psoTFOs. Our results demonstrated that UV irradiation was able to generate psoralen photoadducts through the targeting of the psoTFO to the DNA duplex. By cross-comparison of UV irradiated products from different 5′-end radioactive labeled DNA duplex targets and subsequent photoreversal reactions, two discrete photoadducts, monoadducts and interstrand cross-

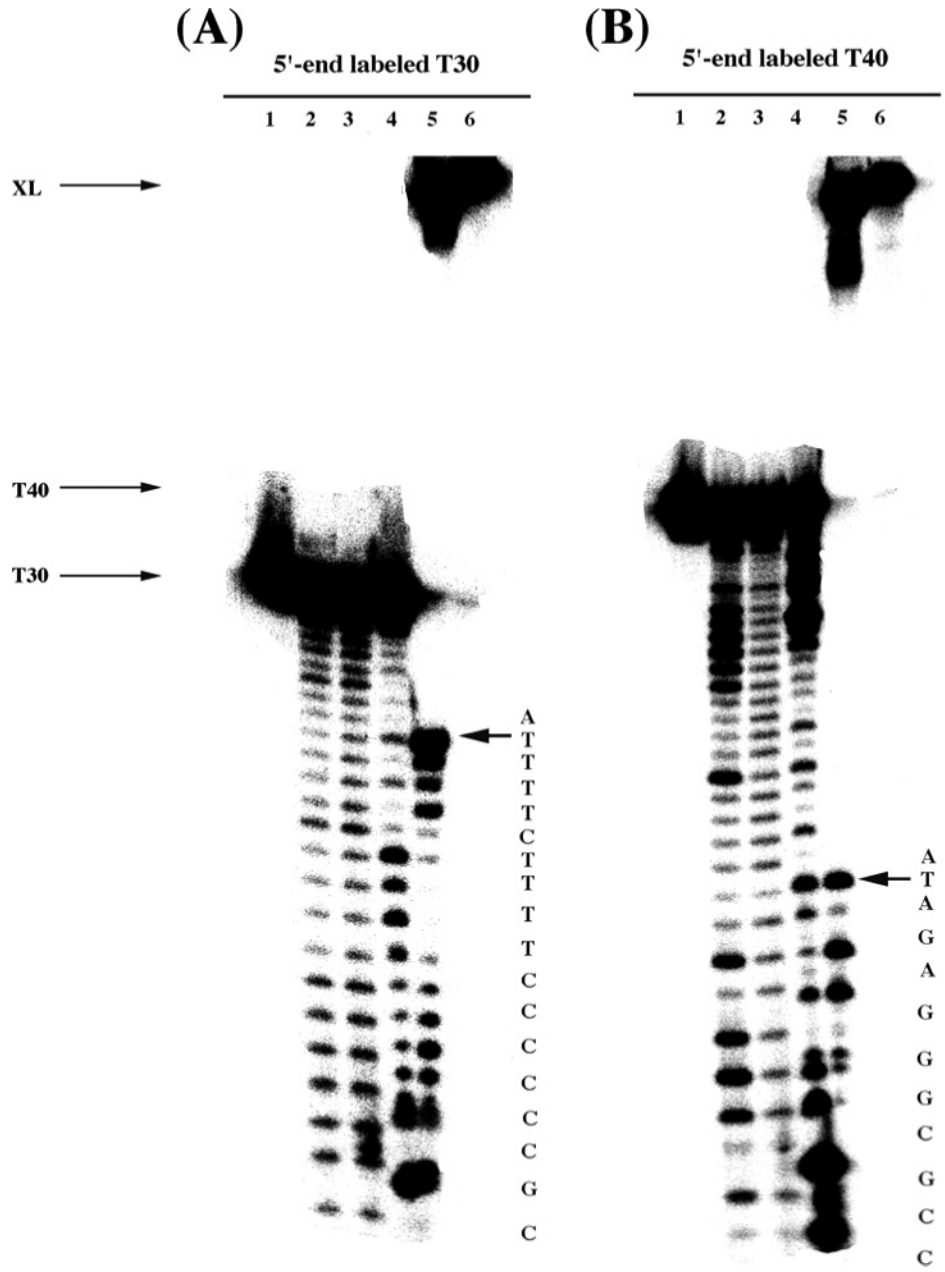

FIGURE 5: Determination of psoralen cross-linking sites by DNase I footprinting. Triplex psoralen-cross-linked products containing the 5′-end radioactive label on the bottom strand, T30 (A) or top strand, T40 (B) of the DNA duplex were purified and partially digested by DNase I, as described in Materials and Methods. Lane 1 shows the un-cross-linked 5′-end labeled strand. Lanes 2 and 3 show Maxam−Gilbert sequencing markers. Lane 2 shows the C reaction (A) and G reaction (B). Lane 3 shows the C+T reaction (A) and A+G reaction (B). Lane 4 shows DNase I treatment of an un-cross-linked strand. Lane 5 shows DNase I digested psoralen cross-links. Lane 6 shows gel-purified psoralen cross-links without DNase I digestion. A gap in the sequence indicates the cross-linking site.

links, were identified. The psoTFOs used in these studies varied in length and interestingly, the ratio of interstrand cross-links and monoadducts formed by the three psoTFOs varied among the three psoTFOs. The varying length of the psoTFO changes the position of psoralen on the DNA duplex and suggests that P14 psoTFO places psoralen only near 5′-TpA-3′ sites of T30 while psoralens conjugated with P15 and P17 psoTFOs are close to 5′-TpA-3′ sites at both strands of the duplex. This placement of psoralen on the duplex would explain why P14 psoTFO formed monoadducts with T30 as major products and P15 and P17 psoTFOs formed interstrand cross-links as major products.

Our cross-linking and DNA footprinting studies are consistent with previous studies that psoralen preferentially targets to 5′-TpA-3′ sites of a DNA duplex (*45*, *46*). The rate of formation of photoadducts among the three psoTFOs is also different. Psoralen interstrand cross-linking is the rate-limiting step for complete psoralen reactivity (*47*) and P14 psoTFO only gives rise to monoadducts with the T30 strand, suggesting that the low yield of cross-links for P14 psoTFO is due to the psoralen being positioned away from the reactive site on the T40 strand. Taken together, our data strongly suggest that the lengths of psoTFO determine the intercalated position of psoralen on a DNA duplex target, influencing the cross-linking efficiencies of psoTFOs.

In addition to establishing the rate of formation of interstrand cross-links, the kinetic experiments showed that the formation of monoadducts occurred preferentially with one of the double strands over the other. For instance, P15 psoTFO first gave rise to monoadducts with the T40 strand

rather than with the T30 strand. On the other hand, the P14 photoreaction with the duplex formed a monadduct with the T30 strand as a major photoproduct. Interestingly, P17 probe formed an interstrand cross-link as a major product. However, why there was a preference for one strand over the other for monoadduct formation was not intuitively obvious. There should be an equal opportunity for both strands of the duplex to form monoadducts with psoralen because the sequence of the cross-linking site for P15 psoTFO contains 5′-TpA/ApT-5′ (Figure 5). Thus, the sequence of the two strands at this specific site should be virtually indistinguishable. We suggest three possibilities to explain these results: (a) Since our psoralen-containing third strands are forming a parallel intermolecular pyr·pur−pyr triplex structural motif, the polypyrimidine third strand is organized asymmetrically in the major groove placing the psoralen moiety in close proximity to the 5′TpA site on the T30 strand for P14 and to the 5′TpA site on the T40 strand for P15 and P17. (b) Second, the sequences flanking the cross-linking site may influence which target site is preferred by psoralen, an effect that is supported by several studies (*5*, *43*). (c) Another possibility is that the flexibility of the DNA conformation may be restricted by the bound TFO during monoadduct formation. Previous studies have shown that a conformational change on the order of 1 μs following monoadduct formation is required in order for cross-linking to take place (*48*, *49*). Once the monoadduct has formed, however, the contribution of the TFO to the conformation of the complex is minimal (*47*).

Previous studies have demonstrated that psoTFO can be used to inhibit transcriptional elongation using sequence-directed targeting that is followed with UV irradiation (*13*, *33*, *36*). The effects of psoralen cross-linking on transcriptional elongation, however, are still unclear. Our previous in vitro transcription assay showed that the formation of psoralen photoadducts using psoTFOs caused both arrest and termination of RNA Pol II transcription (*37*). P14 psoTFO in forming monoadducts as major products caused most of RNA Pol II elongation complexes to terminate transcription. On the other hand, P15 and P17 psoTFOs that generated interstrand cross-links as major products arrested RNA Pol II complexes on templates. These results showed that interstrand psoralen cross-links arrest elongating RNA Pol II complexes, whereas psoralen monoadducts on the DNA template terminate transcription. We thus conclude that the effect of the photoadducts of psoralen on transcription elongation depends on the type of psoralen cross-link formed, which is a factor that is also influenced by the length of the psoTFO. Altogether, our results provide new insight into the photochemistry of psoralen that has given us an understanding of how DNA damage is created during the UV cross-linking process and how that damage leads to a biological response, including changes in the processivity of transcription elongation.

REFERENCES

1. Felsenfeld, G., and Rich, A. (1989) Studies on the formation of two- and three-stranded polyribonucleotides. 1957, *Biochim Biophys Acta 1000*, 87−98.
2. Frank-Kamenetskii, M. D., and Mirkin, S. M. (1995) Triplex DNA structures, *Annu. Rev. Biochem. 64*, 65−95.
3. Le Doan, T., Perrouault, L., Praseuth, D., Habhoub, N., Decout, J. L., Thuong, N. T., Lhomme, J., and Helene, C. (1987) Sequence-specific recognition, photo-cross-linking and cleavage of the DNA double helix by an oligo-[alpha]-thymidylate covalently linked to an azidoproflavine derivative, *Nucleic Acids Res. 15*, 7749−7760.
4. Moser, H. E., and Dervan, P. B. (1987) Sequence-specific cleavage of double helical DNA by triple helix formation, *Science 238*, 645−650.
5. Radhakrishnan, I., and Patel, D. J. (1994) Solution structure of a pyrimidine.purine.pyrimidine DNA triplex containing T.AT, C+.GC and G.TA triples, *Structure 2*, 17−32.
6. Lee, J. S., Woodsworth, M. L., Latimer, L. J., and Morgan, A. R. (1984) Poly(pyrimidine). poly(purine) synthetic DNAs containing 5-methylcytosine form stable triplexes at neutral pH, *Nucleic Acids Res. 12*, 6603−6614.
7. Xodo, L. E., Manzini, G., Quadrifoglio, F., van der Marel, G. A., and van Boom, J. H. (1991) Effect of 5-methylcytosine on the stability of triple-stranded DNA- -a thermodynamic study, *Nucleic Acids Res. 19*, 5625−5631.
8. Giovannangeli, C., Rougee, M., Garestier, T., Thuong, N. T., and Helene, C. (1992) Triple-helix formation by oligonucleotides containing the three bases thymine, cytosine, and guanine, *Proc. Natl. Acad. Sci. U.S.A. 89*, 8631−8635.
9. Beal, P. A., and Dervan, P. B. (1991) Second structural motif for recognition of DNA by oligonucleotide-directed triple-helix formation, *Science 251*, 1360−1363.
10. Radhakrishnan, I., and Patel, D. J. (1993) Solution structure of a purine.purine.pyrimidine DNA triplex containing G.GC and T.AT triples, *Structure 1*, 135−152.
11. Radhakrishnan, I., de los Santos, C., and Patel, D. J. (1993) Nuclear magnetic resonance structural studies of A. AT base triple alignments in intramolecular purine.purine.pyrimidine DNA triplexes in solution, *J. Mol. Biol. 234*, 188−197.
12. Duval-Valentin, G., Thuong, N. T., and Helene, C. (1992) Specific inhibition of transcription by triple helix-forming oligonucleotides, *Proc. Natl. Acad. Sci. U.S.A. 89*, 504−508.
13. Grigoriev, M., Praseuth, D., Guieysse, A. L., Robin, P., Thuong, N. T., Helene, C., and Harel-Bellan, A. (1993) Inhibition of gene expression by triple helix-directed DNA cross-linking at specific sites, *Proc. Natl. Acad. Sci. U.S.A. 90*, 3501−3505.
14. Young, S. L., Krawczyk, S. H., Matteucci, M. D., and Toole, J. J. (1991) Triple helix formation inhibits transcription elongation in vitro, *Proc. Natl. Acad. Sci. U.S.A. 88*, 10023−10026.
15. Cimino, G. D., Gamper, H. B., Isaacs, S. T., and Hearst, J. E. (1985) Psoralens as photoactive probes of nucleic acid structure and function: organic chemistry, photochemistry, and biochemistry, *Annu. Rev. Biochem. 54*, 1151−1193.
16. Kanne, D., Straub, K., Rapoport, H., and Hearst, J. E. (1982) Psoralen-deoxyribonucleic acid photoreaction. Characterization of the monoaddition products from 8-methoxypsoralen and 4, 5′8-trimethylpsoralen, *Biochemistry 21*, 861−871.
17. Spielmann, H. P., Dwyer, T. J., Sastry, S. S., Hearst, J. E., and Wemmer, D. E. (1995) DNA structural reorganization upon conversion of a psoralen furan-side monoadduct to an interstrand cross-link: implications for DNA repair, *Proc. Natl. Acad. Sci. U.S.A. 92*, 2345−2349.
18. Hearst, J. E. (1988) A photochemical investigation of the dynamics of oligonucleotide hybridization, *Annu. Rev. Phys. Chem. 39*, 291−315.
19. Helene, C. (1991) The anti-gene strategy: control of gene expression by triplex-forming-oligonucleotides, *Anticancer Drug Des. 6*, 569−584.
20. Van Houten, B., Gamper, H., Hearst, J. E., and Sancar, A. (1986) Construction of DNA substrates modified with psoralen at a unique site and study of the action mechanism of ABC excinuclease on these uniformly modified substrates, *J. Biol. Chem. 261*, 14135−14141.
21. Gamper, H. B., Cimino, G. D., and Hearst, J. E. (1987) Solution hybridization of cross-linkable DNA oligonucleotides to bacteriophage M13 DNA. Effect of secondary structure on hybridization kinetics and equilibria, *J. Mol. Biol. 197*, 349−362.
22. Cheng, S., Van Houten, B., Gamper, H. B., Sancar, A., and Hearst, J. E. (1988) Use of psoralen-modified oligonucleotides to trap three-stranded RecA-DNA complexes and repair of these cross-linked complexes by ABC excinuclease, *J. Biol. Chem. 263*, 15110−15117.
23. Cheng, S., Sancar, A., and Hearst, J. E. (1991) RecA-dependent incision of psoralen-cross-linked DNA by (A)BC excinuclease, *Nucleic Acids Res. 19*, 657−663.

24. Miller, P. S., Kipp, S. A., and McGill, C. (1999) A psoralen-conjugated triplex-forming oligodeoxyribonucleotide containing alternating methylphosphonate-phosphodiester linkages: synthesis and interactions with DNA, *Bioconjugate Chem. 10*, 572−577.
25. Miller, P. S., Cassidy, R. A., Hamma, T., and Kondo, N. S. (2000) Studies on anti-human immunodeficiency virus oligonucleotides that have alternating methylphosphonate/phosphodiester linkages, *Pharmacol. Ther. 85*, 159−163.
26. Wang, Z., and Rana, T. M. (1995) Chemical conversion of a TAR RNA-binding fragment of HIV-1 Tat protein into a site-specific cross-linking agent, *J. Am. Chem. Soc. 117*, 5438−5444.
27. Wang, Z., Wang, X., and Rana, T. M. (1996) Protein orientation in the Tat-TAR complex determined by psoralen photocross-linking, *J. Biol. Chem. 271*, 16995−16998.
28. Wang, Z., Shah, K., and Rana, T. M. (2001) Probing Tat peptide-TAR RNA interactions by psoralen photocross-linking, *Biochemistry 40*, 6458−6464.
29. Wassarman, D. A. (1993) Psoralen cross-linking of small RNA in vitro, *Mol. Biol. Rep. 17*, 143−151.
30. Guieysse, A. L., Praseuth, D., Grigoriev, M., Harel-Bellan, A., and Helene, C. (1996) Detection of covalent triplex within human cells, *Nucleic Acids Res. 24*, 4210−6421.
31. Guieysse, A. L., Praseuth, D., Giovannangeli, C., Asseline, U., and Helene, C. (2000) Psoralen adducts induced by triplex-forming oligonucleotides are refractory to repair in HeLa cells, *J. Mol. Biol. 296*, 373−383.
32. Sandor, Z., and Bredberg, A. (1995) Deficient DNA repair of triple helix-directed double psoralen damage in human cells, *FEBS Lett. 374*, 287−291.
33. Wang, G., Chen, Z., Zhang, S., Wilson, G. L., and Jing, K. (2001) Detection and determination of oligonucleotide triplex formation-mediated transcription-coupled DNA repair in HeLa nuclear extracts, *Nucleic Acids Res. 29*, 1801−1807.
34. Havre, P. A., and Glazer, P. M. (1993) Targeted mutagenesis of simian virus 40 DNA mediated by a triple helix-forming oligonucleotide, *J. Virol. 67*, 7324−7331.
35. Havre, P. A., Gunther, E. J., Gasparro, F. P., and Glazer, P. M. (1993) Targeted mutagenesis of DNA using triple helix-forming oligonucleotides linked to psoralen, *Proc. Natl. Acad. Sci. U.S.A. 90*, 7879−7883.
36. Intody, Z., Perkins, B. D., Wilson, J. H., and Wensel, T. G. (2000) Blocking transcription of the human rhodopsin gene by triplex-mediated DNA photo-cross-linking, *Nucleic Acids Res. 28*, 4283−4290.
37. Wang, Z., and Rana, T. M. (1997) DNA damage-dependent transcriptional arrest and termination of RNA polymerase II elongation complexes in DNA template containing HIV-1 promoter, *Proc. Natl. Acad. Sci. U.S.A. 94*, 6688−6693.
38. Faucon, B., Mergny, J. L., and Helene, C. (1996) Effect of third strand composition on the triple helix formation: purine versus pyrimidine oligodeoxynucleotides, *Nucleic Acids Res. 24*, 3181−3188.
39. Szewczyk, J. W., Baird, E. E., and Dervan, P. B. (1996) Cooperative triple-helix formation via a minor groove dimerization domain, *J. Am. Chem. Soc. 118*, 6778−6779.
40. Cimino, G. D., Shi, Y. B., and Hearst, J. E. (1986) Wavelength dependence for the photoreversal of a psoralen-DNA cross-link, *Biochemistry 25*, 3013−3020.
41. Shi, Y. B., and Hearst, J. E. (1987) Wavelength dependence for the photoreactions of DNA-psoralen monoadducts. 1. Photoreversal of monoadducts, *Biochemistry 26*, 3786−3792.
42. Boyer, V., Moustacchi, E., and Sage, E. (1988) Sequence specificity in photoreaction of various psoralen derivatives with DNA: role in biological activity, *Biochemistry 27*, 3011−3018.
43. Gia, O., Magno, S. M., Garbesi, A., Colonna, F. P., and Palumbo, M. (1992) Sequence specificity of psoralen photobinding to DNA: a quantitative approach, *Biochemistry 31*, 11818−11822.
44. Ramaswamy, M., and Yeung, A. T. (1994) The reactivity of 4, 5′, 8-trimethylpsoralen with oligonucleotides containing AT sites, *Biochemistry 33*, 5411−5413.
45. Gamper, H., Piette, J., and Hearst, J. E. (1984) Efficient formation of a cross-linkable HMT monoadduct at the Kpn I recognition site, *Photochem. Photobiol. 40*, 29−34.
46. Zhen, W. P., Buchardt, O., Nielsen, H., and Nielsen, P. E. (1986) Site specificity of psoralen-DNA interstrand cross-linking determined by nuclease Bal31 digestion, *Biochemistry 25*, 6598−6603.
47. Oh, D. H., and Hanawalt, P. C. (2000) Binding and photoreactivity of psoralen linked to triple helix-forming oligonucleotides, *Photochem. Photobiol. 72*, 298−307.
48. Johnston, B. H., Johnson, M. A., Moore, C. B., and Hearst, J. E. (1977) Psoralen-DNA photoreaction: controlled production of mono- and diadducts with nanosecond ultraviolet laser pulses, *Science 197*, 906−908.
49. Johnston, B. H., Kung, A. H., Moore, C. B., and Hearst, J. E. (1981) Kinetics of formation of deoxyribonucleic acid cross-links by 4′-(aminomethyl)-4, 5′, 8-trimethylpsoralen, *Biochemistry 20*, 735−738.

BI0488707